Journal of Biomedicine and Biotechnology

Natural Products for Medicine

Guest Editors: Masa-Aki Shibata, Ikhlas A. Khan,
Munekazu Iinuma, and Tomoyuki Shirai

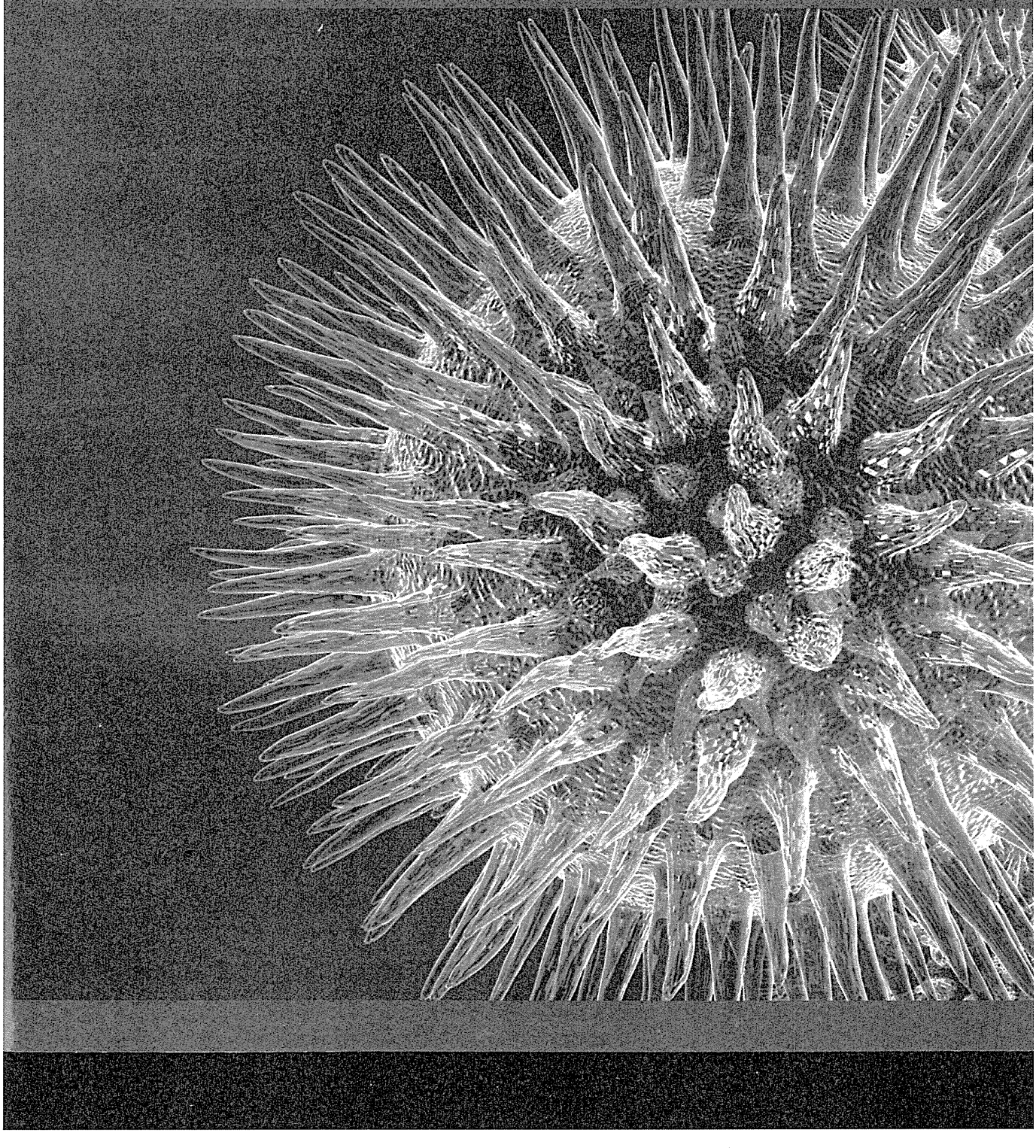

Hindawi Publishing Corporation
Journal of Biomedicine and Biotechnology
Volume 2012, Article ID 147120, 1 page
doi:10.1155/2012/147120

Editorial
Natural Products for Medicine

Masa-Aki Shibata,[1] Ikhlas A. Khan,[2] Munekazu Iinuma,[3] and Tomoyuki Shirai[4]

[1] *Laboratory of Anatomy and Histopathology, Faculty of Health Science, Osaka Health Science University, Osaka 530-0043, Japan*
[2] *Department of Pharmacognosy, School of Pharmacy, University of Mississippi, MS 38677, USA*
[3] *Laboratory of Pharmacognosy, Gifu Pharmaceutical University, Gifu 501-1196, Japan*
[4] *Nagoya City University Graduate School of Medical Sciences, Nagoya 467-8601, Japan*

Correspondence should be addressed to Masa-Aki Shibata, masaaki.shibata@ohsu.ac.jp

Received 15 March 2012; Accepted 15 March 2012

Copyright © 2012 Masa-Aki Shibata et al. This is an open access article distributed under the Creative Commons Attribution License, which permits unrestricted use, distribution, and reproduction in any medium, provided the original work is properly cited.

Throughout human history, natural products—including terrestrial plants, animal products, marine organisms, and products of microorganismal fermentation—have been used in traditional medicines. This historical experience with natural products as therapeutic agents has evolved to sophisticated isolation of active chemical entities from ethnopharmacological plants with the effect that, in modern medicine, natural products are increasingly the primary sources in early drug discovery.

The population is aging in many modern societies and is linked to steadily increasing morbidity rates of cancer and cerebrovascular disease, thus mandating the importance of better preventive as well as therapeutic options. Many medically advanced societies are exploring the adjunctive use of western and oriental medicine alternatives, enhancing the demand for natural products. While evidence-based data is still scant in the field of alternative medicines, in this special issue we have the pleasure of sharing with our readers many scientific articles on natural products with potential medicinal use.

This special issue contains 6 review articles and 19 original peer-reviewed papers. The reviews included summarize such diverse topics as the biological and pharmacological effects of ginsenoside Rb1, isolated from red ginseng root, on skin damage (Y. Kimura et al.); tumor suppression in animals by a fruit pulp containing high amounts of β-cryptoxanthin and hesperidin (T. Tanaka et al.); the favorable effects of purple corn flower in treatment of infectious diseases (J. B. Hudson); the biomechanisms and clinical outcome of *Rhus verniciflia* extract in patients (W. Choi et al.); the safety of cruciferous plant extracts (O. Scott et al.); and the antitumor activity of artemisinin and its analogs (M. P. Crespo-Ortiz and M. Q. Wei). The original articles embrace a wide variety of topics, such as apoptosis, suppression of cell proliferation and tumorigenesis (Y. Hu et al., H. Kurose et al., A. Lerner et al., Booth et al., Kita et al., Mohd et al., and G. M. Geetha et al.), the antibacterial/antifungal/anti-inflammation/antioxidative characteristics of natural extracts (E. Biazar et al., Y.-S. Lee et al., Y. Hu et al., A. Cha et al., H. Sun et al., and P.-F. Kao et al.), cardiovascular activity of specific natural products (K. Awang et al.), the effects of extracts on blood parameter levels in diabetic patients (T. Klangjareonchai and C. Roongpisuthipong), examination of isolation techniques (N. A. Mahyudin et al.), enzymatic activity (B. Elya et al.) and metabolism of certain extracts (Y. Shimoda et al.); and specific effects of some natural products on aryl hydrocarbon receptor expression (H. M. Korashy et al.).

We would like to thank the authors for their timely contributions. Finally, we also thank all reviewers for their hard work questioning, pruning, and refining these articles.

Masa-Aki Shibata
Ikhlas A. Khan
Munekazu Iinuma
Tomoyuki Shirai

Hindawi Publishing Corporation
Journal of Biomedicine and Biotechnology
Volume 2012, Article ID 672428, 9 pages
doi:10.1155/2012/672428

Research Article

Alterations in Cell Cycle and Induction of Apoptotic Cell Death in Breast Cancer Cells Treated with α-Mangostin Extracted from Mangosteen Pericarp

Hitomi Kurose,[1] Masa-Aki Shibata,[2] Munekazu Iinuma,[3] and Yoshinori Otsuki[1]

[1] *Division of Life Sciences, Department of Anatomy and Cell Biology, Osaka Medical College, 2-7 Daigaku-machi, Takatsuki, Osaka 569-8686, Japan*
[2] *Laboratory of Anatomy and Histopathology, Faculty of Health Science, Osaka Health Science University, 1-9-27 Temma, Kita-ku, Osaka 530-0043, Japan*
[3] *Laboratory of Pharmacognosy, Faculty of Pharmacy, Gifu Pharmaceutical University, 1-25-4 Daigaku-nishi, Gifu 501-1196, Japan*

Correspondence should be addressed to Yoshinori Otsuki, an1001@art.osaka-med.ac.jp

Received 31 July 2011; Revised 2 November 2011; Accepted 20 November 2011

Academic Editor: Ikhlas A. Khan

Copyright © 2012 Hitomi Kurose et al. This is an open access article distributed under the Creative Commons Attribution License, which permits unrestricted use, distribution, and reproduction in any medium, provided the original work is properly cited.

The development of molecularly targeted drugs has greatly advanced cancer therapy, despite these drugs being associated with some serious problems. Recently, increasing attention has been paid to the anticancer effects of natural products. α-Mangostin, a xanthone isolated from the pericarp of mangosteen fruit, has been shown to induce apoptosis in various cancer cell lines and to exhibit antitumor activity in a mouse mammary cancer model. In this study, we investigated the influence of α-mangostin on apoptosis and cell cycle in the human breast cancer cell line MDA-MB231 (carrying a p53 mutation, and HER2, ER, and PgR negative) in order to elucidate its anticancer mechanisms. In α-mangostin-treated cells, induction of mitochondria-mediated apoptosis was observed. On cell-cycle analysis, G1-phase arrest, increased $p21^{cip1}$ expression and decreases in cyclins, cdc(s), CDKs and PCNA were observed. In conclusion, α-mangostin may be useful as a therapeutic agent for breast cancer carrying a p53 mutation and having HER2- and hormone receptor-negative subtypes.

1. Introduction

Various molecularly targeted drugs against a range of cancers, including breast cancer, have recently been developed. Trastuzumab is a monoclonal antibody against human epidermal growth factor (HER/ErbB) receptor 2 (HER2/ErbB2). Around 15–20% of patients with breast cancer have HER2-positive tumors, and overexpression of HER2 is observed in these patients [1]. Trastuzumab has been shown to induce tumor regression in such patients. Sunitinib, sorafenib, and bevacizumab are multitargeted tyrosine kinase inhibitors that inhibit tumor neovascularization and are currently in clinical trials [2, 3]. These drugs are associated with serious problems such as adverse effects, drug resistance, and low efficacy of single therapy, particularly against metastatic or recurrent breast cancer. Hormone therapy has also been used against hormone receptor-positive breast cancer. However, about 10 to 15% of breast cancers do not express either estrogen or progesterone receptor (ER and PgR, resp.) and do not overexpress the HER2 gene [4].

Mangosteen (*Garcinia mangostana* Linn) pericarp contains various phytochemicals, primarily xanthones, and the resin extracts have long been used for medicinal purposes in Southeast Asia [5]. α-Mangostin is a one of xanthones present in mangosteen pericarp (78% content). A recent study has shown that α-mangostin induces cell-cycle arrest and apoptosis in various types of human cancer cells [5–8]. We previously reported that α-mangostin significantly inhibits both tumor growth and metastasis in a mouse model of mammary cancer [9, 10]. In addition, α-mangostin treatment significantly decreased the levels of phospho-Akt-threonine 308(Thr308) in a human mammary carcinoma cell line and mammary carcinoma tissues *in vivo* [10].

Here, we investigated the antitumor potential of α-mangostin on apoptosis and cell cycle arrest in a human breast cancer cell line carrying a p53 mutation and having HER2-, ER-, and PgR-negative status.

2. Materials and Methods

2.1. Experimental Regimen. Mangosteen (*Garcinia mangostana* Linn) pericarps were dried, ground, and successively extracted in water and 50% ethanol. After freeze-drying the 50% ethanol extract, the resultant dried powder was suspended in water partitioned with ethyl acetate. The ethyl acetate extract was then purified by chromatography on silica gel with the n-hexane-ethyl acetate system and recrystallized to give α-mangostin at >98% purity. For *in vitro* use, crystallized α-mangostin was dissolved in dimethyl sulphoxide (DMSO), and aliquots of stock 20 mM solution were stored at −20°C.

2.2. Cell Line. The MDA-MB231, a human mammary carcinoma cell line stably expressing the green fluorescence protein (GFP) [11], was maintained in RPMI-1640 medium containing 10% fetal bovine serum with streptomycin/penicillin in an incubator under 5% CO_2. MDA-MB231 cells have a p53 mutation [12, 13] and HER2-, ER-, and PgR, negative feature [14].

2.3. Cell Viability. MDA-MB231 cells were grown in RPMI-1640 medium supplemented with 10% bovine serum under an atmosphere of 95% air and 5% CO_2 at 37°C. These cells were plated into 96-well plates (1×10^4 cells/well) one day before α-mangostin treatment. They were subsequently incubated for 24 h with culture medium containing DMSO vehicle alone (control) or with medium containing α-mangostin at various concentrations up to 48 μM. Cell viability was determined using a Cell-Titer-Bule Cell Viability Assay (Promega Co., Madison, WI, USA). The IC_{50} under these conditions was found to be 20 μM α-mangostin for 24 h treated and 16 μM for 48 h treated in MDA-MB231 cells; thus, all *in vitro* studies were performed using 20 μM α-mangostin.

2.4. Time-Lapse Imaging. Cells were grown on 35 mm culture dishes under the above-mentioned condition. These cells were subsequently incubated for 24 h with culture medium containing DMSO vehicle alone (control) or with medium containing 20 μM α-mangostin. Imaging has started when the reagents were added into dishes. Time-lapse images were taken using the fluorescence microscope BZ8000 (Keyence, Osaka, Japan).

2.5. Nuclear Staining. For nuclear staining, DAPI with mounting medium (Vector Laboratories, Inc., Burlingame, CA, USA) was used after immunofluorescence staining. For morphological examination of apoptotic changes, Hoechst33342 (Lonza Walkersville, Inc., Walkersville, MD, USA) was added to cultured medium at a concentration of 5 μg/mL.

2.6. Caspase Activity. MDA-MB231 cells were plated into 96-well plates at a concentration of 1×10^4 cells/well one day before α-mangostin treatment. Cells were treated with 20 μM α-mangostin or DMSO alone for 24 h. The activities of caspase-3, caspase-8, caspase-9, and caspase-4 were measured using a Fluorometric Protease Assay Kit (MBL, Inc., Nagoya, Japan) in which cells were lysed with Cell Lysis Buffer contained in this kit and the protein concentration adjusted to 50 μg in each sample. Caspase activity was measured in terms of fluorescence intensity produced by caspase cleavage of the corresponding substrate, using Fluoroskan Ascent (Thermo Election Co., Helsinki, Finland).

2.7. Cell-Cycle Distribution. Flow cytometric analysis was conducted on trypsinized MDA-MB231 cell suspensions that were harvested after a 24 h treatment with 20 μM α-mangostin and fixed in cold 70% ethanol. The cells were stained with a 50 μg/mL propidium iodide solution containing 100 μg/mL RNase A for 20 min at 37°C and then placed on ice just prior to flow cytometric analysis (EPICS Elite ESP; Coulter Co., Miami, FL, USA). The percentage of cells in each phase of the cell cycle was determined using a Multicycle Cell-Cycle Analysis program (Coulter Co.).

2.8. ssDNA Analysis. MDA-MB231 cells were plated into 96-well plates at a concentration of 1×10^4 cells/well one day before α-mangostin treatment. Cells were treated with 20 μM α-mangostin or DMSO alone for 24 h. Single-Strand break DNA (ssDNA) levels were detected by using ApoStrand ELISA Apoptosis Detection Kit (Enzo Life Sciences International, Inc., Butler Pike Plymouth Meeting, PA, USA) and measured using Microplate reader (Corona ELECTRIC Co. Ltd., Ibaraki, Japan).

2.9. Cytochrome c Release. Cytochrome *c* leaving the mitochondrial membrane was measured using the InnoCyte Flow Cytometric Cytochrome *c* Release Kit (Merck; Darmstadt, Germany). MDA-MB231 cells were harvested after a 24 h treatment with 20 μM α-mangostin or DMSO alone and 1×10^6 cells were resuspended in 300 μL Permeabilization Buffer to remove the cytosolic cytochrome *c*. The cells were fixed 4% paraformaldehyde and washed. After treatment with blocking buffer, the cells were treated with anticytochrome *c* mouse monoclonal antibody (clone 7H8, Santa Cruz, Biotechnology, CA, USA), followed by secondary antibody conjugated to FITC. Then, the cells were analyzed using a flow cytometer, BD FACSAria (Becton Dickinson, Franklin Lakes, NJ, USA).

2.10. Immunofluorescence Staining. MDA-MB231 cells were grown on 24 mm × 24 mm cover glasses and fixed in 4% formaldehyde solution in phosphate buffer. Immunofluorescence staining was performed with anti-PCNA mouse monoclonal antibody (clone PC10; Cell Signaling Technology, Danvers, MA, USA), cyclin D1 rabbit monoclonal antibody (clone 92G2; Cell Signaling Technology), $p21^{cip1}$ rabbit polyclonal antibody (clone C-19; Santa Cruz Biotechnology). These antibodies were also used in Western blotting.

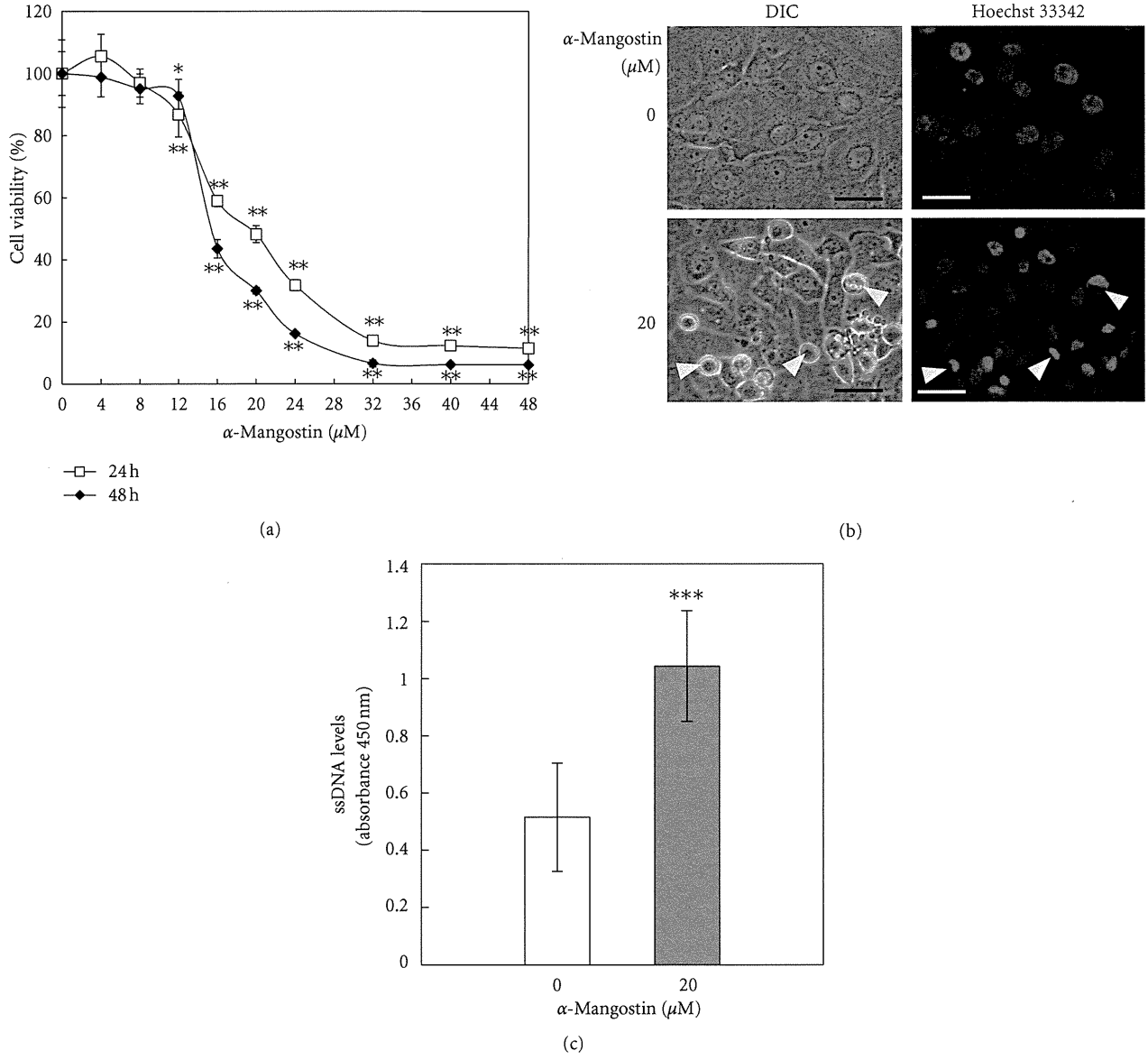

FIGURE 1: Cell viability and apoptosis detection in MDA-MB231 cells after α-mangostin treatment. (a) Cell viability was significantly lower in human mammary carcinoma MDA-MB231 cells treated with more than 12 μM α-mangostin for 24 or 48 h (*$P < 0.05$, **$P < 0.01$). Five samples from each of α-mangostin dosage were examined. The IC_{50} concentration was determined to be 20 μM for 24 h; therefore, 20 μM α-mangostin was used for all *in vitro* studies. (b) Morphological changes in MDA-MB231 cells treated with 20 μM α-mangostin for 24 h, as compared to controls. Upper two panels show controls and lower two panels show α-mangostin-treated cells. α-Mangostin-treated cells appeared shrunken and chromatin condensation was observed (yellow arrow heads in lower right panel). Scale bars = 50 μm. (c) ssDNA levels were determined by ELISA and were significantly elevated in cells treated with α-mangostin for 24 h, as compared to control levels (***$P < 0.001$). Data are presented as mean ± SD. For all analyses, five samples from control and α-mangostin-treated cells were examined.

2.11. Western Blotting. Total protein was extracted from whole cell lysates of MDA-MB231 cells treated with DMSO or α-mangostin according to the IC_{50} data previously stated. Total protein (40 μg) was fractionated on 16% SDS-PAGE mini gels (TEFCO, Tokyo, Japan) under reducing conditions and transferred to PVDF membranes (Immobilon - P Transfer Membrane, Millipore; Billerica, MA, USA). The membranes were activated in 100% methanol for 15 seconds and incubated with primary antibodies for the following proteins: cytochrome *c*, Bid, PCNA, cyclin D1, $p21^{cip1}$, and β-actin. Membranes were then incubated with the corresponding secondary antibodies conjugated with horseradish peroxidase (HRP). β-Actin (clone N-21) and Full-length Bid (clone FL-195) antibodies were from Santa Cruz Biotechnology. Antibody recognizing cleaved Bid was obtained from R&D Systems (R&D Systems, Inc, Minneapolis, MN, USA). Antibody binding was subsequently visualized by exposure to an enhancing chemiluminescence reagent (Amersham ECL;

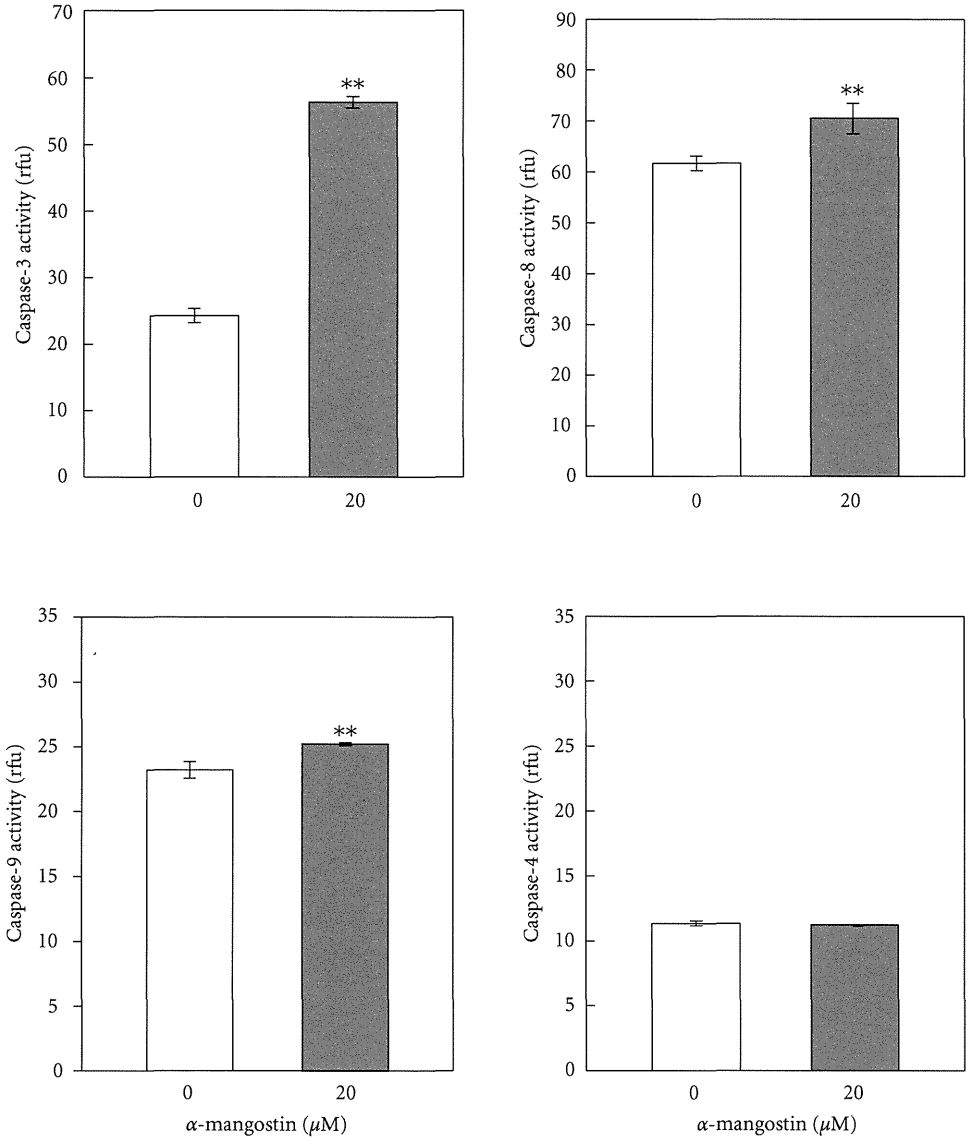

FIGURE 2: Caspase activity of MDA-MB231 cells after treatment with α-mangostin. Caspase activity was evaluated by luminescence assay. Activity of caspase-3, caspase-8, and caspase-9, but not caspase-4, was significantly elevated in MDA-MB231 cells treated with 20 μM α-mangostin for 24 h (**$P < 0.01$). Data are presented as mean ± SD. Five samples from control and α -mangostin-treated cells were used for measurement of caspase activity.

GE Healthcare UK Ltd., Buckinghamshire, UK). Blots were visualized using a LAS-3000 image analyzer (Fujifilm, Co., Tokyo, Japan).

2.12. Real-Time PCR. MDA-MB231 cells were treated with DMSO or 20 μM α-mangostin for 6, 12, and 24 h. Protein was extracted using cell lysis buffer containing protease and phosphatase inhibitor cocktail. Total RNA was extracted from these cells with FastPure RNA kit (Takara Bio Inc., Shiga, Japan) and cDNAs were synthesized with PrimeScript RT reagent kit (Takara Bio Inc.). Primers involved in the cell-cycle regulation were used containing PrimerArray Cell cycle (human) (Takara Bio Inc.) and real-time PCR reaction was performed with Thermal Cycler Dice Real Time (Takara Bio Inc.). Data were corrected against glyceraldehyde-3-phosphate dehydrogenase (GAPDH) values and expressed as mean ± SD.

2.13. Statistical Analysis. Significant differences in the quantitative data between groups were analyzed using Student's *t*-test via the method of Welch, and *P* values less than 0.05 were considered to represent a statistically significant difference.

3. Results and Discussion

3.1. Cell Viability. Viability analyses of MDA-MB231 human mammary cancer cells showed significantly lower viability

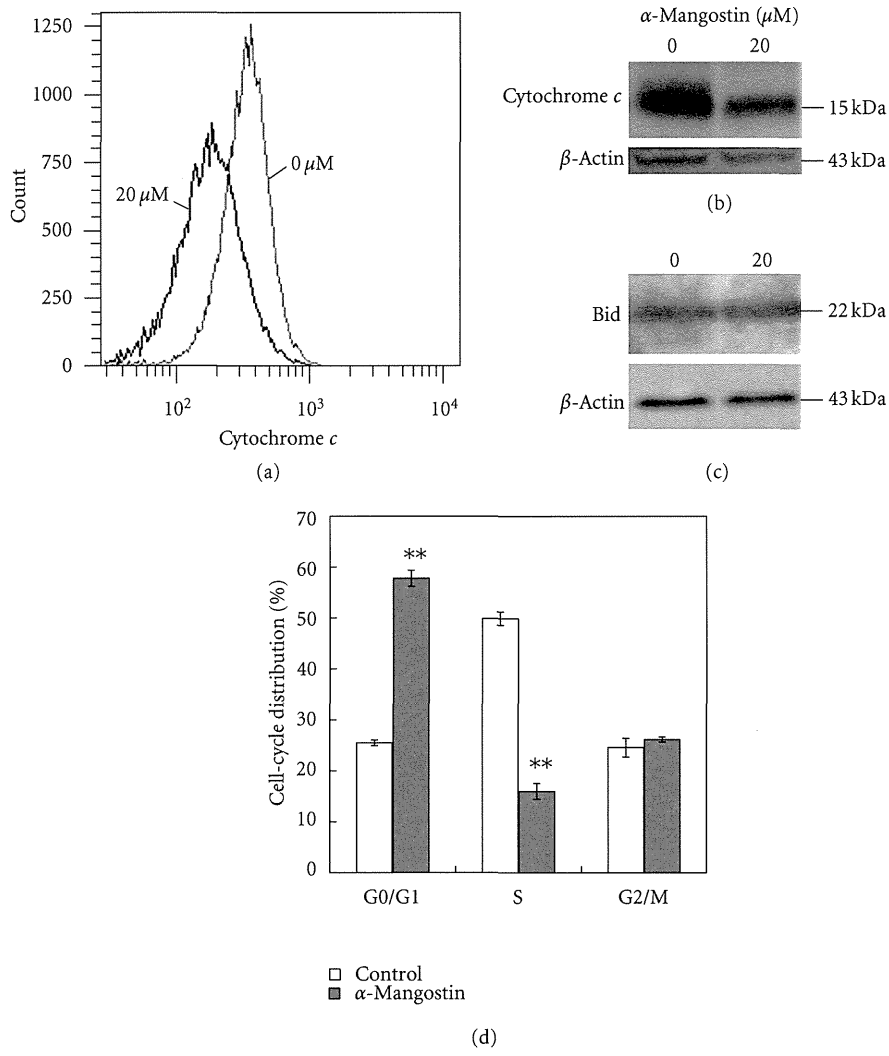

FIGURE 3: Cytochrome *c* expression, Bid cleavage, and cell-cycle distribution of MDA-MB231 cells after α-mangostin treatment. (a) Cytochrome *c* in mitochondria, as determined by flow cytometry (black line indicates α-mangostin-treated cells and gray line indicates controls). The levels of cytochrome *c* protein in mitochondrial fractions were significantly lower in cells treated with α-mangostin for 24 h (b). Western blots of cytochrome *c* (15 kDa) showed significant decreases in cells treated with α-mangostin for 24 h, as compared to controls (upper panel). In α-mangostin-treated cells, cytochrome *c* was released from mitochondria, leading to decreases in concentration. β-Actin served as an internal control (lower panel, same in (c)). (c) Western blots of Bid (22 kDa) in control cells and cells treated with α-mangostin for 24 h were similar (upper panel). Cleaved Bid was not observed after α-mangostin treatment. Three samples were used for all analyses in (a)–(c). (d) Cell-cycle analysis confirmed that α-mangostin induced arrest in the G1-phase and inhibition of cells entering the S-phase in MDA-MB231 cells (**$P < 0.01$). Data are presented as mean ± SD of triplicate, independent measurements.

after 24 and 48 h of treatment with more than 12 μM α-mangostin (Figure 1(a)). Based on the IC_{50} data, 20 μM was determined to be the optimal concentration of α-mangostin for *in vitro* studies.

3.2. Morphological Changes. For morphological examination of apoptotic changes, MDA-MB231 cells were stained with Hoechst 33342 (Figure 1(b)). After 20 μM α-mangostin treatment for 24 h, cells appeared shrunken and chromatin condensation was observed (yellow arrow heads in lower right panel). These changes suggest that the antiproliferative effects of α-mangostin are associated with apoptosis in MDA-MB231 human mammary cancer cells. Furthermore, we performed time-lapse imaging from the start of 20 μM α-mangostin treatment for 24 h. After 6 h, cell proliferation started to decrease significantly and cell shape had changed after 12 h (data not shown).

3.3. Apoptosis Studies

3.3.1. ssDNA Analysis. In order to confirm that the morphological changes observed after α-mangostin treatment occurred as a consequence of apoptosis, we measured ssDNA levels of α-mangostin treated cells, as compared to controls. In α-mangostin-treated cells, ssDNA levels were significantly elevated ($P < 0.001$, Figure 1(c)). This suggests that the

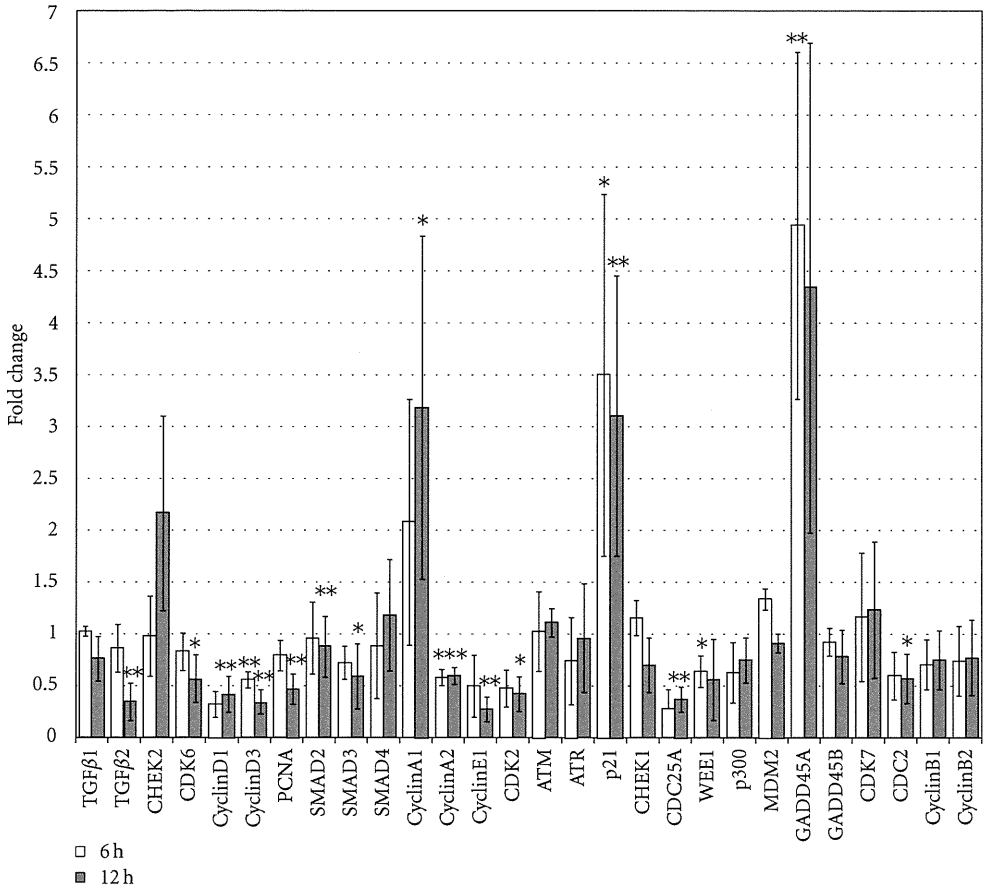

FIGURE 4: Real-time PCR analysis of gene expression associated with cell cycle. mRNA expression of cell-cycle-related genes, such as cyclins, cdc(s), CDKs, and PCNA, was examined by real-time PCR assay in MDA-MB231 cells after treatment with α-mangostin, as compared with controls. White bars and gray bars show the results of analysis for 6 h and 12 h after treatment with 20 μM α-mangostin, respectively ($^*P < 0.05$, $^{**}P < 0.01$). Relative levels of target gene expression were calculated using the $\Delta\Delta$ CT method. GAPDH was used as a reference gene. Data are presented as means $\pm$ SD of triplicate independent measurements.

morphological changes in human mammary cancer cells that occurred after α-mangostin treatment were caused by apoptosis.

3.3.2. Caspase Activity. Significantly elevated caspase-3, caspase-8, and caspase-9 activity was observed in MDA-MB231 cells treated with α-mangostin for 24 h (Figure 2), as compared to controls. The activity of caspase-4 did not differ significantly between control cells and α-mangostin-treated cells (Figure 2). These results indicate that α-mangostin-induced mitochondria mediated apoptosis.

3.3.3. Cytochrome c Release. In order to confirm mitochondria-mediated apoptosis, levels of cytochrome *c* were measured by flow cytometry and Western blot. The levels of cytochrome *c* protein in mitochondrial fractions were significantly lower in cells treated with α-mangostin for 24 h (Figure 3(a)). Cytochrome *c* protein was released from mitochondria, leading to decreases in concentration (Figure 3(b)). These results were strongly suggesting engagement of the mitochondria-mediated apoptotic pathway.

3.3.4. Bid Cleavage. As caspase-8 activity was elevated, we examined whether the mitochondrial pathway was activated via caspase-8-Bid cleavage by performing Western blots for Bid. Full-length Bid (22 kDa) was equally detected in control cells and in cells treated with α-mangostin for 24 h (Figure 3(c)); this indicates that no Bid cleavage occurred. In addition, no cleaved Bid (15 kDa) was observed when using cleaved Bid-detectable antibody in any of the groups (data not shown). These results suggest that apoptosis was induced by α-mangostin via mitochondria, but was not accompanied by Bid cleavage. We previously reported that α-mangostin decreased phospho-Akt-Th308 in MDA-MB231 cells and mammary carcinoma tissues [10]. Akt is a serine/threonine protein kinase that mediates the downstream effects of phosphatidylinositol 3-kinase (PI3K) by phosphorylating multiple targets involved in regulating diverse cellular functions, including proliferation, growth, and survival. Therefore, Akt phosphorylation by therapeutic agents leads to growth inhibition, cell-cycle arrest, and apoptosis in cancer cells. A previous study in human colon cancer cells showed that α-mangostin inhibited Erk1/2

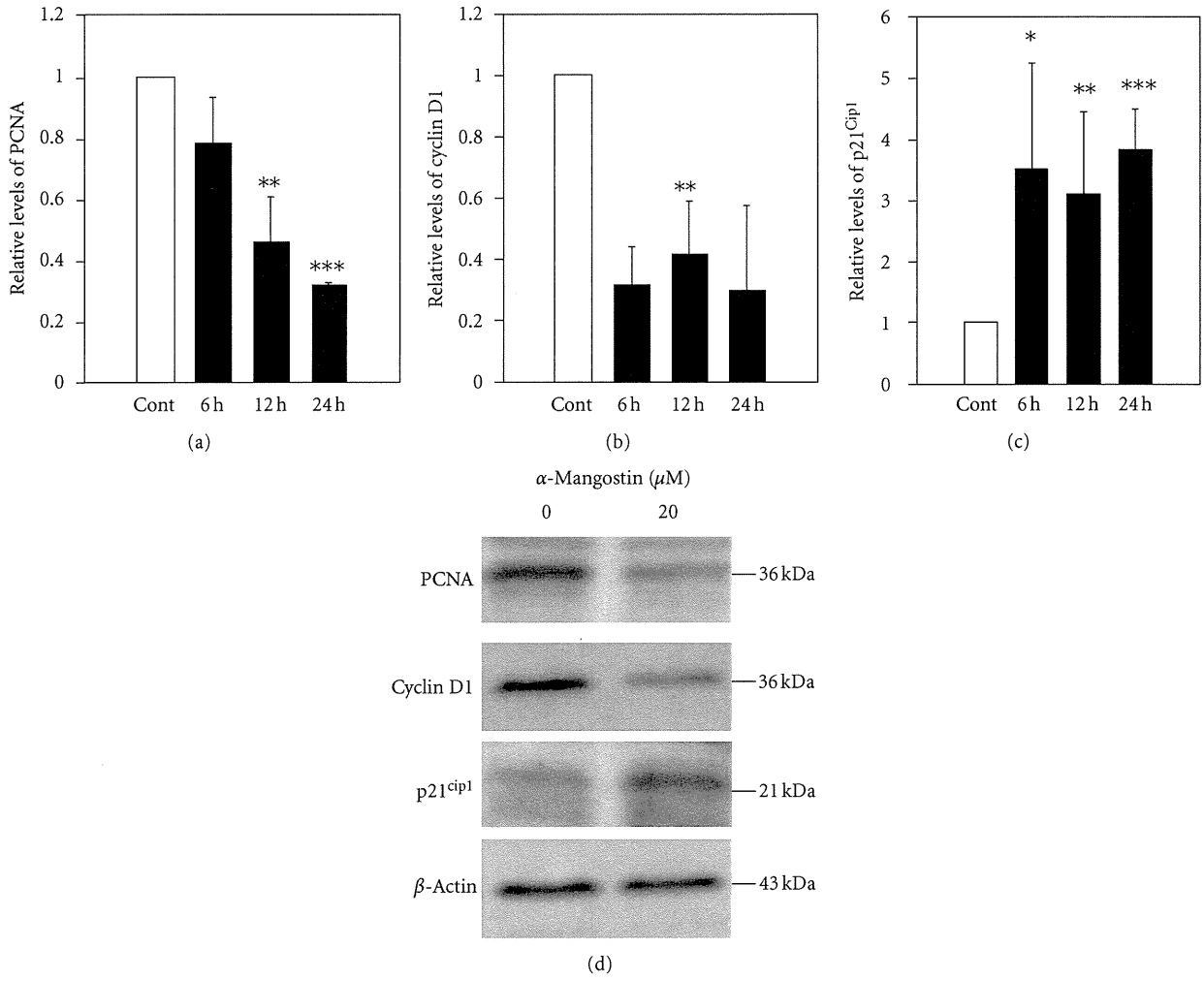

FIGURE 5: Changes in expression of genes involved in G1 phase regulation. (a)–(c) mRNA expressions of cell-cycle regulators for G1 phase, PCNA (a), cyclin D1 (b), and $p21^{cipl}$ (c), were examined using real-time PCR assays in MDA-MB231 cells after treatment with α-mangostin, as compared to controls. White bars indicate the results for controls and black bars indicate the results of analysis at 6 h, 12 h, and 24 h after treatment with α-mangostin ($^*P < 0.05$, $^{**}P < 0.01$). PCNA and cyclin D1 expressions were significantly lower and $p21^{cipl}$ was significantly higher in cells treated with α-mangostin for 24 h, as compared to controls. Relative target gene levels were calculated using the $\Delta\Delta$CT method. GAPDH was used as a reference gene. Data are presented as means ± SD of triplicate independent measurements. (d) Western blots of PCNA (36 kDa) and cyclin D1 (36 kDa) showed significantly lower levels, and $p21^{cipl}$ (21 kDa) showed significantly higher levels in cells treated with α-mangostin for 24 h, as compared to controls (left lane). These results were similar to those for PCR analysis, as shown in (a)–(c). β-Actin served as an internal control (lowest panel). Three samples from control and α-mangostin-treated cells were used for measurement.

and Erk5 phosphorylation involving the mitogen-activated protein kinase (MAPK) signaling pathway [5]. PI3K/Akt and Erk signaling target Bcl-2-associated agonists of cell death (Bad), a member of the Bcl-2 family. Bcl-2 family members are known to be regulators of programmed cell death. Bad promotes apoptosis by displacing Bax, another Bcl-2 family member, from binding to Bcl-2 and Bcl-xL, causing cytochrome *c* release from mitochondria [15]. These data suggest that apoptotic cell death caused by α-mangostin treatment in human mammary carcinoma cells occurs via mitochondria-mediated apoptosis, followed by inhibition of PI3K/Akt signaling pathway, and may include Bad activation.

3.4. Cell-Cycle Distribution. As measured by flow cytometry, 24 h exposure to 20 μM α-mangostin induced a significant elevation in the number of cells in the G1-phase, as compared with control cells (Figure 3(d)). There was also a significant reduction in the S-phase population in α-mangostin-treated cells (Figure 3(d)). These results suggest that G1-phase arrest was the result of α-mangostin inhibiting entry into S-phase.

3.5. Expression of Cell-Cycle Regulatory Genes. As α-mangostin treatment induced cell-cycle arrest, we investigated the expression of cell-cycle regulatory genes. Real-time analysis revealed that the expression of $p21^{cipl}$ was up-regulated and CHEK2 expression tended to increase for more than 6 h after α-mangostin treatment (Figure 4). $p21^{cipl}$ is a cyclin-dependent kinase inhibitor and the encoded protein binds to and inhibits the activity of cyclin-CDK2 (CDK: cyclin-dependent kinase) or -CDK4 complexes, thereby functioning

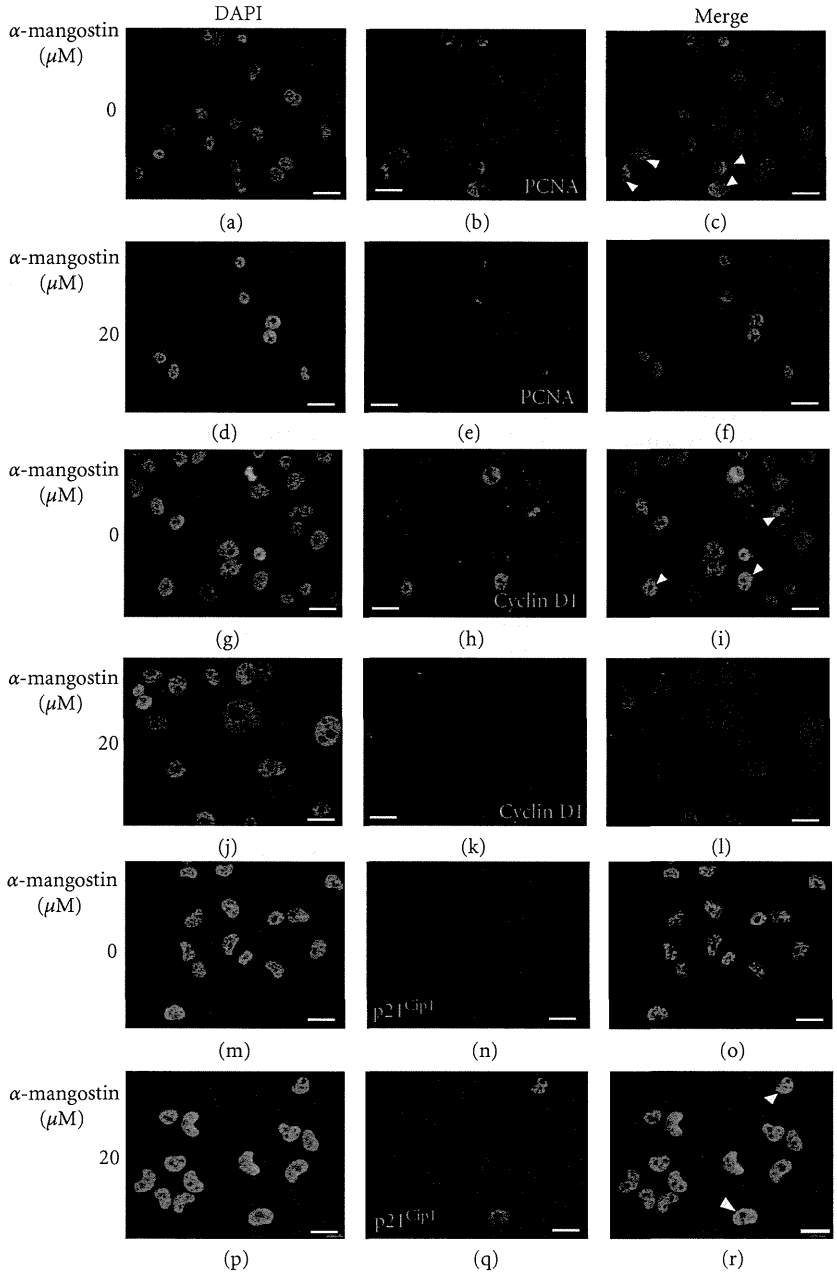

FIGURE 6: Expression of PCNA, cyclin D1 and $p21^{cip1}$ proteins after α-mangostin treatment. Immunofluorescence of PCNA (a)–(f), cyclin D1 (g)–(l), and $p21^{cip1}$ (m)–(r) in MDA-MB231 cells after 24 h of treatment with α-mangostin ((d)–(f), (j)–(l), (p)–(r)), as compared with controls ((a)–(c), (g)–(i), (m)–(o)). Yellow arrowheads in panels (c), (i), and (r) indicate higher expression of each protein in nuclei. PCNA and cyclin D1 expression was reduced and $p21^{cip1}$ expression were elevated in α-mangostin-treated cells, as compared to controls. Scale bars = 25 μm.

as a regulator of cell-cycle progression at the G1-phase [16]. CHEK2 is one of the cell-cycle checkpoint regulators and putative tumor suppressors that lead to G1-phase arrest through CDK phosphatase and cell division cycle 25 homolog A (cdc25A) phosphorylation [17]. Increases in $p21^{cip1}$ and CHEK2 expression lead to decreases in CDKs and cyclins, and G1-phase arrest and inhibition of cell proliferation, followed by decreases in proliferating cell nuclear antigen (PCNA). Furthermore, we confirmed the expression of G1/S-phase-related molecules, particularly $p21^{cip1}$, PCNA, and cyclin D1 by using Western blotting and immunofluorescence staining (Figures 5 and 6). On Western blotting analysis, PCNA (36 kDa) and cyclin D1 (36 kDa) protein were significantly lower, and $p21^{cip1}$ (21 kDa) protein was significantly elevated in cells treated with α-mangostin for 24 h, as compared to controls (Figure 5(d)). These results agreed with those of the real-time PCR analysis shown in Figures 4 and 5(a)–5(c). Immunofluorescence staining

revealed that PCNA and cyclin D1 expression were lower and that $p21^{cip1}$ expression was elevated in the nuclei of α-mangostin-treated cells, as compared to controls (Figure 6). These results suggest that α-mangostin induces G1-phase arrest and S-phase suppression by altering the expression of cell-cycle-related molecules, such as $p21^{cip1}$, CHEK2, cyclins, cdc(s), CDKs, and PCNA.

4. Conclusion

In conclusion, our results demonstrated that the therapeutic effects of α-mangostin are mediated by mitochondria-mediated apoptosis under control of the PI3K/Akt signaling pathway. α-Mangostin may be useful as a therapeutic agent for breast cancer carrying a p53 mutation and including HER2/hormone-negative subtypes.

Acknowledgments

This investigation involved Industry-Academic-Government collaboration as follows: PM Riken-yakka Ltd., Field & Device Co., Osaka Health Science University, Osaka Medical Collage, Gifu Pharmaceutical University, and a Grant-in-Aid for Private Universities from the Ministry of Education, Culture, Sports, Science and Technology of Japan. The authors thank Mr. Teruo Ueno (the Central Research Laboratory of Osaka Medical Collage) for assistance with the cell-cycle analysis.

References

[1] J. Baselga, D. Tripathy, J. Mendelsohn et al., "Phase II study of weekly intravenous trastuzumab (Herceptin) in patients with HER2/neu-overexpressing metastatic breast cancer," *Seminars in Oncology*, vol. 26, no. 4, supplement 12, pp. 78–83, 1999.

[2] H. Wildiers, C. Fontaine, P. Vuylsteke et al., "Multicenter phase II randomized trial evaluating antiangiogenic therapy with sunitinib as consolidation after objective response to taxane chemotherapy in women with HER2-negative metastatic breast cancer," *Breast Cancer Research and Treatment*, vol. 123, no. 2, pp. 463–469, 2010.

[3] N. S. Azad, E. M. Posadas, V. E. Kwitkowski et al., "Combination targeted therapy with sorafenib and bevacizumab results in enhanced toxicity and antitumor activity," *Journal of Clinical Oncology*, vol. 26, no. 22, pp. 3709–3714, 2008.

[4] K. R. Bauer, M. Brown, R. D. Cress, C. A. Parise, and V. Caggiano, "Descriptive analysis of estrogen receptor (ER)-negative, progesterone receptor (PR)-negative, and HER2-negative invasive breast cancer, the so-called triple-negative phenotype: a population-based study from the California Cancer Registry," *Cancer*, vol. 109, no. 9, pp. 1721–1728, 2007.

[5] Y. Akao, Y. Nakagawa, M. Iinuma, and Y. Nozawa, "Anti-cancer effects of xanthones from pericarps of mangosteen," *International Journal of Molecular Sciences*, vol. 9, no. 3, pp. 355–370, 2008.

[6] K. Matsumoto, Y. Akao, H. Yi et al., "Preferential target is mitochondria in α-mangostin-induced apoptosis in human leukemia HL60 cells," *Bioorganic and Medicinal Chemistry*, vol. 12, no. 22, pp. 5799–5806, 2004.

[7] P. Moongkarndi, N. Kosem, S. Kaslungka, O. Luanratana, N. Pongpan, and N. Neungton, "Antiproliferation, antioxidation and induction of apoptosis by Garcinia mangostana (mangosteen) on SKBR3 human breast cancer cell line," *Journal of Ethnopharmacology*, vol. 90, no. 1, pp. 161–166, 2004.

[8] K. Matsumoto, Y. Akao, K. Ohguchi et al., "Xanthones induce cell-cycle arrest and apoptosis in human colon cancer DLD-1 cells," *Bioorganic and Medicinal Chemistry*, vol. 13, no. 21, pp. 6064–6069, 2005.

[9] H. Doi, M. A. Shibata, E. Shibata et al., "Panaxanthone isolated from pericarp of Garcinia mangostana L. suppresses tumor growth and metastasis of a mouse model of mammary cancer," *Anticancer Research*, vol. 29, no. 7, pp. 2485–2495, 2009.

[10] M. A. Shibata, M. Iinuma, J. Morimoto et al., "α-Mangostin extracted from the pericarp of the mangosteen (Garcinia mangostana Linn) reduces tumor growth and lymph node metastasis in an immunocompetent xenograft model of metastatic mammary cancer carrying a p53 mutation," *BMC Medicine*, vol. 9, article 69, 2011.

[11] M. A. Shibata, Y. Miwa, J. Morimoto, and Y. Otsuki, "Easy stable transfection of a human cancer cell line by electrogene transfer with an Epstein-Barr virus-based plasmid vector," *Medical Molecular Morphology*, vol. 40, no. 2, pp. 103–107, 2007.

[12] J. Bartek, R. Iggo, J. Gannon, and D. P. Lane, "Genetic and immunochemical analysis of mutant p53 in human breast cancer cell lines," *Oncogene*, vol. 5, no. 6, pp. 893–899, 1990.

[13] P. M. O'Connor, J. Jackman, I. Bae et al., "Characterization of the p53 tumor suppressor pathway in cell lines of the National Cancer Institute anticancer drug screen and correlations with the growth-inhibitory potency of 123 anticancer agents," *Cancer Research*, vol. 57, no. 19, pp. 4285–4300, 1997.

[14] Y. Liang, J. Wu, G. M. Stancel, and S. M. Hyder, "P53-dependent inhibition of progestin-induced VEGF expression in human breast cancer cells," *Journal of Steroid Biochemistry and Molecular Biology*, vol. 93, no. 2–5, pp. 173–182, 2005.

[15] E. Yang, J. Zha, J. Jockel, L. H. Boise, C. B. Thompson, and S. J. Korsmeyer, "Bad, a heterodimeric partner for Bcl-x(L), and Bcl-2, displaces Bax and promotes cell death," *Cell*, vol. 80, no. 2, pp. 285–291, 1995.

[16] Y. Xiong, G. J. Hannon, H. Zhang, D. Casso, R. Kobayashi, and D. Beach, "p21 is a universal inhibitor of cyclin kinases," *Nature*, vol. 366, no. 6456, pp. 701–704, 1993.

[17] J. Falck, N. Mailand, R. G. Syljuåsen, J. Bartek, and J. Lukas, "The ATM-Chk2-Cdc25A checkpoint pathway guards against radioresistant DNA synthesis," *Nature*, vol. 410, no. 6830, pp. 842–847, 2001.

Med Mol Morphol (2012) 45:179–184
DOI 10.1007/s00795-012-0576-5

© The Japanese Society for Clinical Molecular Morphology 2012

REVIEW

Masa-Aki Shibata · Jayakrishna Ambati · Eiko Shibata
Katsuhide Yoshidome · Mariko Harada-Shiba

Mammary cancer gene therapy targeting lymphangiogenesis: VEGF-C siRNA and soluble VEGF receptor-2, a splicing variant

Received: March 2, 2012 / Accepted: March 14, 2012

Abstract Metastasis contributes significantly to cancer mortality, and the most common pathway of initial dissemination is via the afferent ducts of the lymphatics. Overexpression of vascular endothelial growth factor (VEGF)-C has been associated with lymphangiogenesis and lymph node metastasis in a multitude of human neoplasms, including breast cancers. We recently reported that both VEGF-C siRNA and endogenous soluble vascular endothelial growth factor receptor-2 (esVEGFR-2, a new splicing variant) inhibit VEGF-C function and metastasis in a mouse model of metastatic mammary cancer. Here we briefly review our previous experimental work, specifically targeting tumor lymphangiogenesis, in which metastatic mouse mammary cancers received direct intratumoral injections of either expression vectors VEGF-C siRNA or esVEGFR-2, or the empty plasmid vector, once a week for 6 or 8 weeks, followed by in vivo gene electrotransfer of the injected tumors. Throughout our study, both tumor lymphangiogenesis and the multiplicity of lymph node metastasis were significantly inhibited, with an overall reduction in tumor growth, by both VEGF-C siRNA and csVEGFR-2; further, a significant reduction in the number of dilated lymphatic vessels containing intraluminal cancer cells was observed with both treatments. Thus, therapeutic strategies targeting lymphangiogenesis may have great clinical significance for the treatment of metastatic human breast cancer.

M-A. Shibata (✉)
Laboratory of Anatomy and Histopathology, Faculty of Health Science, Osaka Health Science University, 1-9-27 Temma, Kita-ku, Osaka 530-0043, Japan
Tel. +81-6-7506-9046; Fax +81-6-6352-5995
e-mail: masaaki.shibata@ohsu.ac.jp

J. Ambati
Department of Ophthalmology and Visual Science and Physiology, University of Kentucky, Lexington, KY, USA

E. Shibata · M. Harada-Shiba
Department of Molecular Innovation in Lipidology, National Cerebral & Cardiovascular Center Research Institute, Osaka, Japan

K. Yoshidome
Department of Breast Cancer and Endocrine Surgery, Graduate School of Medicine, Osaka University, Suita, Osaka, Japan

Key words VEGF-C · siRNA · Soluble VEGFR-2 · Lymphangiogenesis · Mammary cancer metastasis

Introduction

Breast cancer is the most common malignant disease in women, with more than 1000000 cases and 370000 deaths occurring worldwide annually.[1] In Japan, the incidence of breast cancer is continuously increasing, the number of deaths, rising 2.6 fold between 1970 and the early 2000s, with the disease now ranking fifth as a cause of female mortality.[2] Perhaps more worrisome is the apparently increasing incidence of breast cancer among younger women, under 40 years of age, recently reported in many countries worldwide.[3–5] The lethality of breast cancer is largely the result of metastasis, which occurs preferentially in the lymph nodes, lungs, and bones.[6] To delay disease progression and prolong patient life, more effective preventive and antimetastatic treatments combined with less toxic chemotherapeutic agents are desperately required.

Cancer cells spread through the body by different mechanisms, such as direct invasion of surrounding tissue, dispersion of cells via the blood vascular system (hematogenous metastasis), or dissemination by means of the lymphatic system (lymphatic metastasis). Although vascular endothelial growth factor-C (VEGF-C) is normally expressed in tissues such as large intestine, mammary duct, prostate, thyroid, ovary, and cardiac and skeletal muscle,[7] it is also expressed in a variety of malignant tumors including mammary neoplasm[8] and, additionally, has been shown to play a major role in lymphangiogenesis. High levels of VEGF-C expression have been reported to be associated with lymph node metastasis and poor prognosis in patients with breast cancer.[9,10] A number of animal studies using cell lines derived from various cancers[11–13] and transgenic mice overexpressing or underexpressing VEGF-C[14] have been conducted to demonstrate that VEGF-C overexpression promotes cancer metastasis.

In 2009, Ambati's group found an endogenous soluble isoform of VEGFR-2 (esVEGFR-2), which plays a crucial

role in maintaining the alymphatic cornea in mice.[15] This isoform is a truncated 230-kDa membrane-bound form of VEGFR-2 resulting from alternative splicing and is a specific inhibitor of lymphatic vessel growth by VEGF-C sequestration.[15] Tissue-specific loss of esVEGFR-2 in mice at birth induces spontaneous lymphatic invasion of the normally alymphatic cornea and dermal lymphatic hyperplasia without affecting angiogenesis. Treatment with esVEGFR-2 inhibits lymphangiogenesis, but not angiogenesis, induced by corneal suture injury or transplantation and enhances corneal allograft survival; esVEGFR-2 also suppresses cell proliferation in lymphangioma.[15]

Within the past few years, RNA interference has become the most widely used technology for gene silencing. A popular therapeutic concept involves knockdown of VEGF-C expression by gene silencing using vectors expressing short interfering RNA (siRNA) to suppress mammary cancer metastasis by vascular spread. The more recently discovered esVEGFR-2 , which exhibits selective inhibition of VEGF-C signaling, might offer another therapeutic tool for preventing cancer metastasis. In this small review, we demonstrate inhibitory effects on lymph node metastasis by both VEGF-C siRNA[16] and esVEGFR-2[17] in an immunocompetent mouse mammary cancer model having a metastatic spectrum similar to that seen in human breast cancers.

Mammary cancer gene therapy using VEGF-C siRNA

BJMC3879 cell line

The BJMC3879 cell line was derived from a metastatic focus within a lymph node of a BALB/c mouse originally inoculated with purified MMTV virus obtained from the media in which Jyg-MC cells, established from mammary tumors of the Chinese wild mouse, were grown.[18] Mammary tumors developing in syngeneic mice injected with BJMC3879 cells show a high metastatic propensity, especially to lymph nodes and lungs.[19,20] This cell line and the tumors resulting from its inoculation not only express both VEGF-C (Fig. 1A) and VEGFR-3[20] but also contain p53 mutation (Fig. 1B).[21–23]

In vivo siRNA gene therapy targeting VEGF-C

The VEGF-C siRNA sequence and the plasmid vector details are reported elsewhere.[16] In this study, BJMC3879 cells were injected into the right inguinum of female BALB/c mice. Within 2 weeks of cell inoculation, tumors developed into which we directly injected psiRNA-VEGF-C or control psiRNA-SCR (which contains a scramble sequence that presents no homology with any human or mouse mRNA), followed immediately by in vivo gene electrotransfection. The vectors were injected using a 27-gauge needle at a concentration of 0.5 μg/μl in sterile saline while the animals were under isoflurane anesthesia. A total volume of 150 μl was introduced into larger tumors, while smaller tumors of 0.6–0.7 cm were infused until we detected leakage of the vector solution; we estimated that this method delivered 50–75 μg plasmid, depending on tumor size. Gene electrotransfer was accomplished with 8 pulses of 20 ms each at 100 V delivered directly to the tumor via platinum plate electrodes "forceps" connected to a CUY21EDIT square-wave electropulser (Nepa Gene, Chiba, Japan).

Tumor growth and lymph node metastasis in VEGF-C siRNA gene therapy

Using calipers, we measured the size of each treated mammary tumor weekly and calculated tumor volumes using the formula *maximum diameter* × *(minimum diameter)*^{2} × *0.4*.[24] After 8 weeks of treatment, all mice were killed and the mammary tumors, selected lymph nodes (i.e., lymph nodes from axillary and femoral regions as well as any that appeared abnormal), and lungs were removed and portions immediately fixed in 10% phosphate-buffered formalin. Fixed tissue sections were processed through to paraffin embedding, cut at 4 μm, and stained with hematoxylin and eosin (H&E) for histopathological examination.

Suppression of tumor growth, as inferred by computed volume, was evident in the psiRNA-VEGF-C group from week 2 on when compared to the psiRNA-SCR group, with significant reduction in tumor volumes from weeks 3 to 7. Histopathologically, the mammary tumors proved to be moderately differentiated adenocarcinomas. All control mice treated with psiRNA-SCR developed metastasis to the lymph nodes, whereas only half the psiRNA-VEGF-C-tranfected mice showed lymph node metastases. Further, the multiplicity of lymph node metastases per mouse was also significantly lower in the psiRNA-VEGF-C group compared to the siRNA-SCR control mice.

Lymphatic and blood microvascular density in mammary tumors

We employed avidin–biotin complex immunohistochemistry to quantitatively assess lymphatic and blood microvessel density in the primary mammary carcinomas. Prepared tumor sections were stained with hamster anti-podoplanin monoclonal antibody as a marker for lymphatic endothelium (AngioBio, Del Mar, CA, USA), and with rabbit polyclonal anti-CD31 (Lab Vision, Fremont, CA, USA), a specific marker for blood vessel endothelium. The numbers of podoplanin-positive lymphatic vessels containing intraluminal tumor cells were counted and expressed as an average ± SD; the numbers of CD31-positive blood microvessels were also counted as previously described.[25]

In all groups, lymphatic microvessels were well developed in the outer, superficial layers of mammary tumors in a somewhat hexagonal network pattern. Tumor cells were frequently observed within the lumina of dilated lymphatic vessels (Fig. 1A,C) in both control and treated tumors, but the number of affected lymphatic vessels was significantly lower in the psiRNA-VEGF-C versus psiRNA-SCR group. Similarly, the numbers of CD-31-positive microvessels were also significantly lower in the psiRNA-VEGF-C.

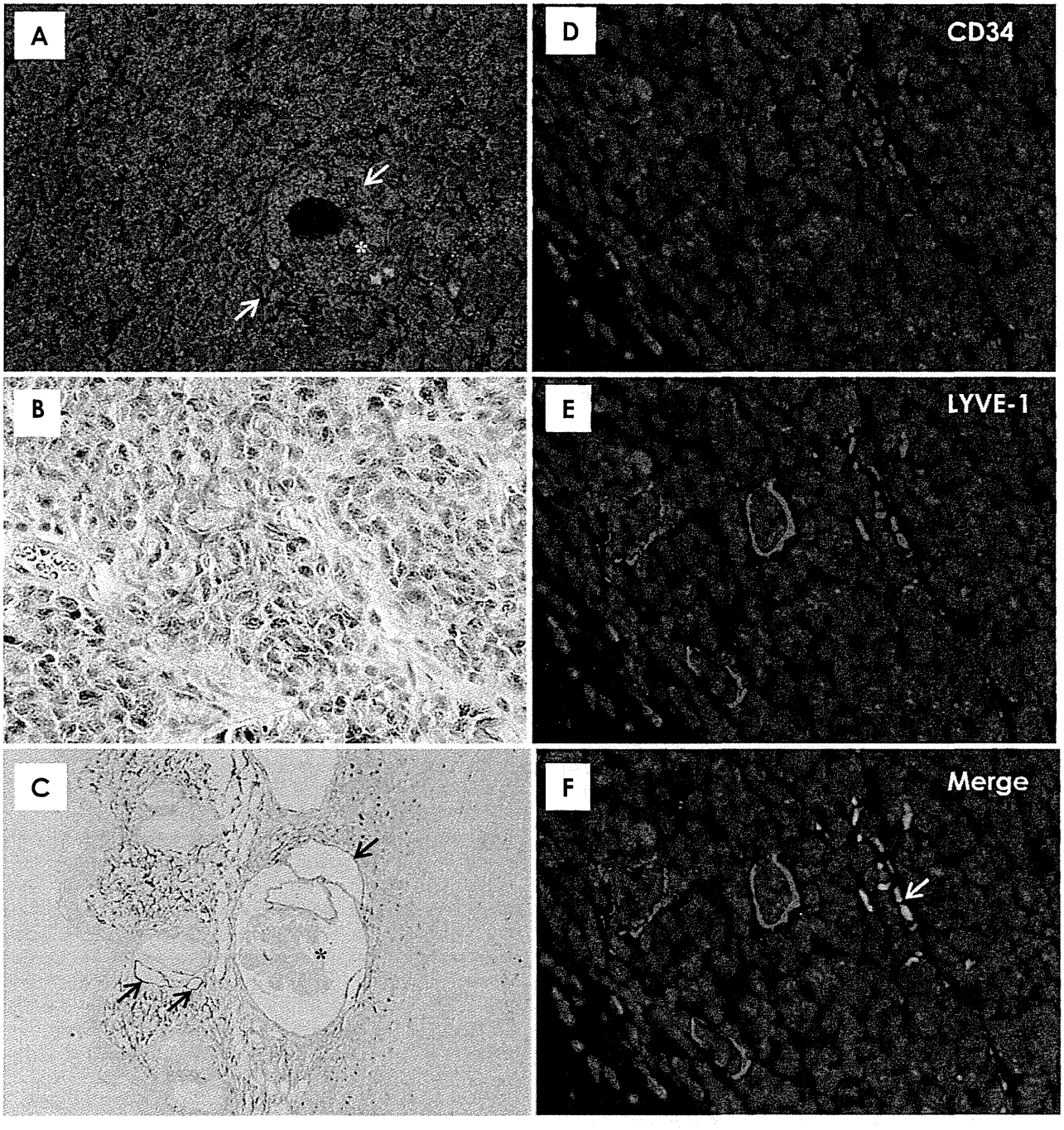

Fig. 1. A Strong expression of vascular endothelial growth factor (VEGF)-C (*green*; Alexa-488) was observed in mammary carcinoma induced by BJMC3879 cell inoculation. Lymphatic microvessels (*red*; Texas red, *arrows*) were contained intraluminal cancer cells (*asterisk*). Immunofluorescence histochemistry (goat anti-precursor VEGF-C antibody and hamster anti-podoplanin antibody). DAPI nuclear staining. ×400. **B** Note *brownish* nuclear staining for abnormal p53 protein, indicating that these cancer cells carry mutant p53. p53 immunohistochemistry (Pab240 anti-p53 antibody reacts to the mutant protein in formalin-fixed paraffin-embedded specimens). ×400. **C** Podoplanin-positive lymphatic microvessels (*arrows*) of a carcinoma were often dilated and filled with invading carcinoma cells (*asterisk*). Podoplanin immunohistochemistry (hamster anti-podoplanin antibody). ×100. **D–F** Double immunofluorescence histochemical staining with CD34 for blood microvessels (*red*; Alexa-594) (**D**) and LYVE-1 for lymphatic microvessels (*green*; Alexa-488) (**E**) and their merged images (**F**) in BJMC3879 mammary carcinomas. An *arrow* in the merged image (**F**) shows microvessels expressing both molecules CD34 and LYVE-1 ($CD34^+/LYVE\text{-}1^+$ microvessels). Immunofluorescence histochemistry (rat anti-CD34 antibody and rabbit anti-LYVE-1 antibody). DAPI nuclear staining. ×400

Mammary cancer gene therapy using esVEGFR-2

Cell line and animal model

The experimental design was similar to the VEGF-C siRNA study, with a few exceptions such as the cell line used and the shorter experimental period (6 vs. 8 weeks). In this study, we used the BJMC3879luc2 mammary carcinoma cell line, which is stably transfected with the *luc2* gene, an improved *firefly luciferase* gene.[26] Overexpression of esVEGFR-2 in tumors was achieved by inserting the open reading frame of *esVegfr2*, cloned from mouse corneal cDNA, into a pcDNA3.1 vector as previously described.[15] Empty vector pcDNA3.1 was used as a control vector and referred to as pVec. BJMC3879luc2 cells were again inoculated into the right inguinum of female BALB/c mice and the resulting tumors transfected in vivo using gene electrotransfer (described in the previous section) of either pesVEGFR-2 or pVec. In this study, we also decided to inject all surviving animals with 50 mg/kg 5-bromo-2′-deoxyuridine (BrdU; Sigma, St. Louis, MO, USA) to investigate cell proliferation within fixed, paraffin-embedded tumor samples and to use terminal deoxynucleotidyl transferase-mediated dUTP-FITC nick end-labeling (TUNEL; Wako Pure Chemical Industries, Osaka, Japan) staining to examine apoptosis.

Tumor growth, metastasis, and microvessel densities

As in the previous VEGF-C study, we saw a significant suppression of tumor volume with pesVEGFR-2 treatment from week 2 to study termination as compared to the control pVec group. In this experiment, all mice in both the treated and control groups developed lymph node metastasis; however, the number of lymph node metastases per mouse was significantly lower in the pesVEGFR-2 group as compared to the pVec group.

Immunofluorescence histochemistry (IFH) was performed on samples using the lymphatic and blood microvessel markers LYVE-1 and CD34, respectively, to quantitatively assess the number of microvessels present in primary tumors. Rabbit anti- LYVE-1 (Acris Antibodie, Herford, Germany) and rat anti-CD34 (Hycult Biotech, Uden, Netherland) were used as primary antibodies and were detected using goat anti-rat Alexa-594 and goat anti-rabbit Alexa-488. Nuclear staining was performed with 4′,6-diamidino-2-phenylindole (DAPI). The corresponding three images (CD34, LYVE-1, and DAPI) were merged into a single image, and the number of $CD31^-/LYVE\text{-}1^+$ lymphatic microvessels and the number of $CD31^+/LYVE\text{-}1^-$ blood microvessels were counted (Fig. 1D–F). IFH analysis demonstrated a significant decrease in the number of lymphatic microvessels in tumors transfected with pesVEGFR-2 group as compared to those in pVec controls, whereas the number of blood microvessels was similar in both groups.

We also examined the number of lymphatic vessels containing intraluminal tumor cells using podoplanin as previously described. Number of lymphatic microvessels with migrating cancer cells was significantly decreased with pesVEGFR-2 treatment as compared to pVec.

Cell proliferation and apoptosis

We detected no apparent differences in the number of TUNEL-positive cells (i.e., apoptotic cells) in tumor sections exposed to pesVEGFR-2 or empty vector. However, cell proliferation, as assessed by BrdU immunohistochemistry, was significantly reduced in pesVEGFR-2-treated mammary tumors over control tumors.

Discussion

The metastatic spread of tumor cells is mediated by a number of mechanisms, including direct invasion into local tissue, spread via the lymphatics, or hematogenous dissemination. However, the most common pathway of initial dissemination is via the afferent ducts of the lymphatics,[27] and lymphangiogenesis is considered a key process for lymphatic metastasis. In contrast to angiogenesis, investigations on lymphangiogenesis in tumors are conspicuously lacking, possibly because of the dearth of identified lymphangiogenic factors; without suitable lymphatic endothelial markers, it is impossible to definitively distinguish blood from lymphatic microvessels. The recent discoveries of such lymphatic-specific markers as LYVE-1, podoplanin, and prox-1 have greatly contributed to investigations into lymphangiogenesis and the mechanism of lymphatic metastasis. This understanding should lead, in turn, to adjunctive therapeutic strategies for metastasis prevention/inhibition.

Overexpression of VEGF-C has been associated with lymphatic vessel invasion and lymph node metastasis in a multitude of human cancers, including breast cancers,[8,28] and many animal tumor models have provided direct evidence of a causal role for VEGF-C in tumor lymphangiogenesis and metastasis.[29] In murine mammary cancer models, knockdown of VEGF-C by siRNA suppresses lymph node metastasis.[16,30] It has been shown that the VEGF-C receptor, VEGFR-3, is predominantly expressed on lymphatic endothelial cells,[31] and, further, that VEGF-C-dependent activation of VEGFR-3 induces the growth of those cells.[32] Inhibition of VEGFR-3 signaling by soluble VEGFR-3 (sVEGFR-3) or by blocking antibody inhibits lymph node metastasis in animal tumor models and is associated with an inhibition of lymphangiogenesis, but not of angiogenesis, in tumors.[13,33,34] In contrast, others have reported that VEGFR-3 antibody therapy significantly suppresses both angiogenesis and lymphangiogenesis[35] and that sVEGFR-3 significantly reduces lymphangiogenesis but only slightly inhibits hematogenous vascular formation; the authors of this latter study speculate that the mild inhibition of angiogenesis may have been responsible for the evident delay in the in vivo tumor growth.[36]

In comparison to directly blocking the VEGF-C receptor, recent work with splicing variants has shown that endogenous soluble VEGFR-2 (esVEGFR-2), a VEGF-C

antagonist, is associated with normal alymphatic cornea and shows selective inhibition of lymphangiogenesis.[15] We saw a significant reduction in the multiplicity of lymph node metastasis with esVEGFR-2 treatment coupled to decreased numbers of lymphatic vessels in mammary carcinomas without a detectable decrease in angiogenesis in our mammary tumor model.[17] In both our experiments in this review, we observed a significant decrease in the number of lymphatic vessels containing intraluminal tumor cells in both VEGF-C siRNA and esVEGFR-2-treated groups as compared with controls. This finding indicates an inhibitory effect on migration into tumor lymphatic vessels, corroborating the significant reduction in lymph node metastasis also noted in these groups. In human breast cancer, the histopathological finding of tumor cells in lymphatic vessels has been shown to play a very important role in tumor progression of invasive ductal carcinoma.[37,38]

Previous studies using different tissue models have found that the systemic administration of anti-VEGFR-3 blocking antibody inhibits lymph node metastasis and reduces lymphatic vessel density in orthotopic lung[13] and gastric tumors[33] in nude mice with no changes in angiogenesis or in tumor weight. VEGF-C itself induces tumor growth in orthotopic prostate tumors[39] and in gastric carcinomas[40] in nude mice. Given our results, we question why esVEGFR-2 suppresses tumor growth without suppressing tumor angiogenesis. It should be noted that although we did see a marked reduction in tumor growth and decreased cell proliferation, as determined by BrdU-labeling indices, it came without an increase in apoptosis in the mammary tumors exposed to esVEGFR-2. VEGF-C has shown to induce cell proliferation of tumor cells.[39,40] Because esVEGFR-2 is an effective antagonist of VEGF-C, it is possibly that esVEGFR-2 treatment suppressed tumor growth and BrdU-labeling indices without inhibiting tumor angiogenesis. In addition, the number of $CD8^+$ T cells and dendritic cells is significantly increased in inoculated murine mammary tumor cells stably transfected with VEGF-C siRNA, suggesting that VEGF-C negatively modulates the immune response.[30] Therefore, the immune response may also participate in the antimetastatic potential of VEGF-C siRNA or pesVEGFR-2 in the immunocompetent mammary cancer model in the present experiment.

We have demonstrated that targeting lymphangiogenesis by downregulating VEGF-C through siRNA silencing or by using the antagonistic alternative splicing variant esVEGFR-2 significantly suppresses tumor growth and lymph node metastasis in a mouse mammary cancer model. One can argue that the inhibition of metastasis in these treatments may simply be a reflection of suppressed tumor growth via overall cell proliferation – in human studies, it is generally recognized that once a malignant tumor has reached 4 cm or more, the chance of tumor recurrence and/or metastasis increases dramatically[41] – but we believe it is more likely the combination of decreased cell proliferation coupled to reduced lymphangiogenesis is additively inhibitive to metastasis. As the extent of lymph node involvement is a major criterion for evaluating patient prognosis, we further believe therapeutic strategies targeting lymphangiogenesis may have great clinical significance for the treatment of metastatic human breast cancer.

Acknowledgments This review and our investigations were supported, in part, from a Grant-in-Aid for Science Research (C) (2) from the Ministry of Education, Culture, Sports, Science and Technology of Japan (No. 17591360 and No. 21591682 to M.A. Shibata). This work was also partially supported by Grants-in-Aid for Scientific Research from the Japanese Ministry of Health, Labour and Welfare (H23-seisakutan-saku-ippan-004 to M. Harada-Shiba). We thank Ms. Naomi Nakano (Osaka Health Science University) and Ms. Akiko Yoshida (National Cerebral & Cardiovascular Center Research Institute) for their excellent secretarial assistance.

References

1. Guarneri V, Conte PF (2004) The curability of breast cancer and the treatment of advanced disease. Eur J Nucl Med Mol Imaging 31(suppl 1):S149–S161
2. Kuroishi T, Tominaga S (2001) Epidemiology of breast cancer. Jpn J Cancer Chemother 28:168–173
3. Agarwal G, Pradeep PV, Aggarwal V, Yip CH, Cheung PS (2007) Spectrum of breast cancer in Asian women. World J Surg 31: 1031–1040
4. Brinton LA, Sherman ME, Carreon JD, Anderson WF (2008) Recent trends in breast cancer among younger women in the United States. J Natl Cancer Inst 100:1643–1648
5. Bouchardy C, Fioretta G, Verkooijen HM, Vlastos G, Schaefer P, Delaloye JF, Neyroud-Caspar I, Balmer Majno S, Wespi Y, Forni M, Chappuis P, Sappino AP, Rapiti E (2007) Recent increase of breast cancer incidence among women under the age of forty. Br J Cancer 96:1743–1746
6. Nguyen DX, Massague J (2007) Genetic determinants of cancer metastasis. Nat Rev Genet 8:341–352
7. Joory KD, Levick JR, Mortimer PS, Bates DO (2006) Vascular endothelial growth factor-C (VEGF-C) expression in normal human tissues. Lymphat Res Biol 4:73–82
8. Salven P, Lymboussaki A, Heikkila P, Jaaskela-Saari H, Enholm B, Aase K, von Euler G, Eriksson U, Alitalo K, Joensuu H (1998) Vascular endothelial growth factors VEGF-B and VEGF-C are expressed in human tumors. Am J Pathol 153:103–108
9. Mylona E, Alexandrou P, Mpakali A, Giannopoulou I, Liapis G, Markaki S, Keramopoulos A, Nakopoulou L (2007) Clinicopathological and prognostic significance of vascular endothelial growth factors (VEGF)-C and -D and VEGF receptor 3 in invasive breast carcinoma. Eur J Surg Oncol 33:294–300
10. Nakamura Y, Yasuoka H, Tsujimoto M, Imabun S, Nakahara M, Nakao K, Nakamura M, Mori I, Kakudo K (2005) Lymph vessel density correlates with nodal status, VEGF-C expression, and prognosis in breast cancer. Breast Cancer Res Treat 91:125–132
11. Skobe M, Hawighorst T, Jackson DG, Prevo R, Janes L, Velasco P, Riccardi L, Alitalo K, Claffey K, Detmar M (2001) Induction of tumor lymphangiogenesis by VEGF-C promotes breast cancer metastasis. Nat Med 7:192–198
12. Karpanen T, Egeblad M, Karkkainen MJ, Kubo H, Yla-Herttuala S, Jaattela M, Alitalo K (2001) Vascular endothelial growth factor C promotes tumor lymphangiogenesis and intralymphatic tumor growth. Cancer Res 61:1786–1790
13. He Y, Kozaki K, Karpanen T, Koshikawa K, Yla-Herttuala S, Takahashi T, Alitalo K (2002) Suppression of tumor lymphangiogenesis and lymph node metastasis by blocking vascular endothelial growth factor receptor 3 signaling. J Natl Cancer Inst 94:819–825
14. Mandriota SJ, Jussila L, Jeltsch M, Compagni A, Baetens D, Prevo R, Banerji S, Huarte J, Montesano R, Jackson DG, Orci L, Alitalo K, Christofori G, Pepper MS (2001) Vascular endothelial growth factor-C-mediated lymphangiogenesis promotes tumour metastasis. EMBO J 20:672–682
15. Albuquerque RJ, Hayashi T, Cho WG, Kleinman ME, Dridi S, Takeda A, Baffi JZ, Yamada K, Kaneko H, Green MG, Chappell J, Wilting J, Weich HA, Yamagami S, Amano S, Mizuki N, Alexander JS, Peterson ML, Brekken RA, Hirashima M, Capoor S, Usui T,

Ambati BK, Ambati J (2009) Alternatively spliced vascular endothelial growth factor receptor-2 is an essential endogenous inhibitor of lymphatic vessel growth. Nat Med 15:1023–1030
16. Shibata MA, Morimoto J, Shibata E, Otsuki Y (2008) Combination therapy with short interfering RNA vectors against VEGF-C and VEGF-A suppresses lymph node and lung metastasis in a mouse immunocompetent mammary cancer model. Cancer Gene Ther 15:776–786
17. Shibata MA, Ambati J, Shibata E, Albuquerque RJ, Morimoto J, Ito Y, Otsuki Y (2010) The endogenous soluble VEGF receptor-2 isoform suppresses lymph node metastasis in a mouse immunocompetent mammary cancer model. BMC Med 8:69
18. Morimoto J, Imai S, Haga S, Iwai Y, Iwai M, Hiroishi S, Miyashita N, Moriwaki K, Hosick HL (1991) New murine mammary tumor cell lines. In Vitro Cell Dev Biol 27A:349–351
19. Shibata MA, Morimoto J, Otsuki Y (2002) Suppression of murine mammary carcinoma growth and metastasis by HSV*tk*/GCV gene therapy using *in vivo* electroporation. Cancer Gene Ther 9:16–27
20. Shibata MA, Ito Y, Morimoto J, Kusakabe K, Yoshinaka R, Otsuki Y (2006) In vivo electrogene transfer of interleukin-12 inhibits tumor growth and lymph node and lung metastases in mouse mammary carcinomas. J Gene Med 8:335–352
21. Shibata MA, Akao Y, Shibata E, Nozawa Y, Ito T, Mishima S, Morimoto J, Otsuki Y (2007) Vaticanol C, a novel resveratrol tetramer, reduces lymph node and lung metastases of mouse mammary carcinoma carrying p53 mutation. Cancer Chemother Pharmacol 60:681–691
22. Shibata MA, Morimoto J, Shibata E, Akamatsu K, Kurose H, Li Z-L, Kusakabe M, Ohmichi M, Otsuki Y (2010) Raloxifene inhibits tumor growth and lymph node metastasis in a xenograft model of metastatic mammary cancer. BMC Cancer 10:566
23. Shibata MA, Iinuma M; Morimoto J, Kurose H, Akamatsu K, Okuno Y, Akao Y, Otsuki Y (2011) a-Manogstin extracted from the pericarp of the mangosteen (*Garcinia mangostana* Linn.) reduces tumor growth and lymph node metastasis in an immunocompetent xenograft model of metastatic mammary cancer carrying a p53 mutation. BMC Med 9:69
24. Shibata MA, Liu M-L, Knudson MC, Shibata E, Yoshidome K, Bandy T, Korsmeyer SJ, Green JE (1999) Haploid loss of *bax* leads to accelerated mammary tumor development in C3(1)/SV40-TAg transgenic mice: reduction in protective apoptotic response at the preneoplastic stage. EMBO J 18:2692–2701
25. Gorrin-Rivas MJ, Arii S, Furutani M, Mizumoto M, Mori A, Hanaki K, Maeda M, Furuyama H, Kondo Y, Imamura M (2000) Mouse macrophage metalloelastase gene transfer into a murine melanoma suppresses primary tumor growth by halting angiogenesis. Clin Cancer Res 6:1647–1654
26. Shibata MA, Shibata E, Morimoto J, Eid NAS, Tanaka Y, Watanabe M, Otsuki Y (2009) An immunocompetent murine model of metastatic mammary cancer accessible to bioluminescence imaging. Anticancer Res 29:4389–4396
27. Sleeman JP (2000) The lymph node as a bridgehead in the metastatic dissemination of tumors. Recent Results Cancer Res 157: 55–81
28. Valtola R, Salven P, Heikkila P, Taipale J, Joensuu H, Rehn M, Pihlajaniemi T, Weich H, deWaal R, Alitalo K (1999) VEGFR-3 and its ligand VEGF-C are associated with angiogenesis in breast cancer. Am J Pathol 154:1381–1390
29. Achen MG, Mann GB, Stacker SA (2006) Targeting lymphangiogenesis to prevent tumour metastasis. Br J Cancer 94:1355–1360
30. Chen Z, Varney ML, Backora MW, Cowan K, Solheim JC, Talmadge JE, Singh RK (2005) Down-regulation of vascular endothelial cell growth factor-C expression using small interfering RNA vectors in mammary tumors inhibits tumor lymphangiogenesis and spontaneous metastasis and enhances survival. Cancer Res 65: 9004–9011
31. Kaipainen A, Korhonen J, Mustonen T, van Hinsbergh VW, Fang GH, Dumont D, Breitman M, Alitalo K (1995) Expression of the fms-like tyrosine kinase 4 gene becomes restricted to lymphatic endothelium during development. Proc Natl Acad Sci USA 92:3566–3570
32. Joukov V, Pajusola K, Kaipainen A, Chilov D, Lahtinen I, Kukk E, Saksela O, Kalkkinen N, Alitalo K (1996) A novel vascular endothelial growth factor, VEGF-C, is a ligand for the Flt4 (VEGFR-3) and KDR (VEGFR-2) receptor tyrosine kinases. EMBO J 15:290–298
33. Shimizu K, Kubo H, Yamaguchi K, Kawashima K, Ueda Y, Matsuo K, Awane M, Shimahara Y, Takabayashi A, Yamaoka Y, Satoh S (2004) Suppression of VEGFR-3 signaling inhibits lymph node metastasis in gastric cancer. Cancer Sci 95:328–333
34. Lin J, Lalani AS, Harding TC, Gonzalez M, Wu WW, Luan B, Tu GH, Koprivnikar K, VanRoey MJ, He Y, Alitalo K, Jooss K (2005) Inhibition of lymphogenous metastasis using adeno-associated virus-mediated gene transfer of a soluble VEGFR-3 decoy receptor. Cancer Res 65:6901–6909
35. Laakkonen P, Waltari M, Holopainen T, Takahashi T, Pytowski B, Steiner P, Hicklin D, Persaud K, Tonra JR, Witte L, Alitalo K (2007) Vascular endothelial growth factor receptor 3 is involved in tumor angiogenesis and growth. Cancer Res 67:593–599
36. Burton JB, Priceman SJ, Sung JL, Brakenhielm E, An DS, Pytowski B, Alitalo K, Wu L (2008) Suppression of prostate cancer nodal and systemic metastasis by blockade of the lymphangiogenic axis. Cancer Res 68:7828–7837
37. Hasebe T, Okada N, Iwasaki M, Akashi-Tanaka S, Hojo T, Shibata T, Sasajima Y, Tsuda H, Kinoshita T (2010) Grading system for lymph vessel tumor emboli: significant outcome predictor for invasive ductal carcinoma of the breast. Hum Pathol 41:706–715
38. Hasebe T, Sasaki S, Imoto S, Ochiai A (2002) Characteristics of tumors in lymph vessels play an important role in the tumor progression of invasive ductal carcinoma of the breast: a prospective study. Mod Pathol 15:904–913
39. Tuomela J, Valta M, Seppanen J, Tarkkonen K, Vaananen HK, Harkonen P (2009) Overexpression of vascular endothelial growth factor C increases growth and alters the metastatic pattern of orthotopic PC-3 prostate tumors. BMC Cancer 9:362
40. Kodama M, Kitadai Y, Tanaka M, Kuwai T, Tanaka S, Oue N, Yasui W, Chayama K (2008) Vascular endothelial growth factor C stimulates progression of human gastric cancer via both autocrine and paracrine mechanisms. Clin Cancer Res 14:7205–7214
41. Carter CL, Allen C, Henson DE (1989) Relation of tumor size, lymph node status, and survival in 24740 breast cancer cases. Cancer (Phila) 63:181–187

スプライシング・バリアントである可溶性VEGF受容体2型のマウス乳癌リンパ節転移に対する抑制効果

[1]大阪保健医療大学保健医療学部解剖学・病理組織学研究グループ,
[2]大阪医科大学医学部生命科学講座・解剖学教室,
[3]ケンタッキー大学眼科学・視覚生理学教室,
[4]国立循環器病研究センター研究所病態代謝部, [5]大阪医科大学実験動物センター
柴田　雅朗[1,2], Jayakrishna Ambati[3], 柴田　映子[4], Romulo JC Albuquerque[3],
森本　純司[5], 斯波　真理子[4], 藤岡　重和[1], 伊藤　裕子[2], 大槻　勝紀[2]

Alternatively spliced soluble VEGF receptor-2 isoform suppresses lymph node metastasis in a mouse immunocompetent mammary cancer model

Masa-Aki Shibata[1,2], Jayakrishna Ambati[3], Eiko Shibata[4], Romulo JC Albuquerque[3], Junji Morimoto[5], Mariko Harada-Shiba[4], Shigekazu Fujioka[1], Yuko Ito[2] and Yoshinori Otsuki[2]
[1]Laboratory of Anatomy and Histopathology, Faculty of Health Science, Osaka Health Science University, 1-9-27 Temma, Kita-ku, Osaka, 530-0043, Japan
[2]Division of Life Sciences, Department of Anatomy and Cell Biology, Osaka Medical College, 2-7, Daigaku-machi, Takatsuki, Osaka 569-8686, Japan
[3]Department of Ophthalmology and Visual Sciences and Physiology, University of Kentucky, Lexington, KY, USA
[4]Department of Molecular Innovation in Lipidology, National Cerebral & Cardiovascular Center Research Institute, Suita, Osaka 565-8565 Japan
[5]Laboratory Animal Center, Osaka Medical College, 2-7, Daigaku-machi, Takatsuki, Osaka 569-8686, Japan

リンパ学　第35巻　第1号　別刷
2012年7月31日
(Japanese Journal of Lymphology)
Vol. 35　No. 1, July 2012

スプライシング・バリアントである可溶性VEGF受容体2型のマウス乳癌リンパ節転移に対する抑制効果

[1]大阪保健医療大学保健医療学部解剖学・病理組織学研究グループ,
[2]大阪医科大学医学部生命科学講座・解剖学教室,
[3]ケンタッキー大学眼科学・視覚生理学教室,
[4]国立循環器病研究センター研究所病態代謝部, [5]大阪医科大学実験動物センター
柴田　雅朗[1,2], Jayakrishna Ambati[3], 柴田　映子[4], Romulo JC Albuquerque[3],
森本　純司[5], 斯波　真理子[4], 藤岡　重和[1], 伊藤　裕子[2], 大槻　勝紀[2]

Alternatively spliced soluble VEGF receptor-2 isoform suppresses lymph node metastasis in a mouse immunocompetent mammary cancer model

Masa-Aki Shibata[1,2], Jayakrishna Ambati[3], Eiko Shibata[4], Romulo JC Albuquerque[3], Junji Morimoto[5], Mariko Harada-Shiba[4], Shigekazu Fujioka[1], Yuko Ito[2] and Yoshinori Otsuki[2]
[1]Laboratory of Anatomy and Histopathology, Faculty of Health Science, Osaka Health Science University, 1-9-27 Temma, Kita-ku, Osaka, 530-0043, Japan
[2]Division of Life Sciences, Department of Anatomy and Cell Biology, Osaka Medical College, 2-7, Daigaku-machi, Takatsuki, Osaka 569-8686, Japan
[3]Department of Ophthalmology and Visual Sciences and Physiology, University of Kentucky, Lexington, KY, USA
[4]Department of Molecular Innovation in Lipidology, National Cerebral & Cardiovascular Center Research Institute, Suita, Osaka 565-8565 Japan
[5]Laboratory Animal Center, Osaka Medical College, 2-7, Daigaku-machi, Takatsuki, Osaka 569-8686, Japan

Key words：　VEGF receptor-2, soluble, splicing variant, metastasis, mammary cancer

はじめに

血管内皮増殖因子VEGF（Vascular endothelial growth factor）ファミリーは脈管の発生から新生，また病的な脈管新生に関与している．血管新生はVEGF-AによりVEGF受容体-1（VEGFR-1）やVEGF受容体-2（VEGFR-2）が活性化され引き起こされる．一方，リンパ管新生は主にVEGF-CによりVEGFR-3の活性化により惹起される．最近，可溶性VEGFR-3（sVEGFR-3）やVEGFR-3抗体によってVEGFR-3シグナルを遮断すると，リンパ管新生の減少に伴ってリンパ節転移が抑制されると報告されている．2009年，本稿の共著者の一人であるAmbatiらのグループは内因性の可溶性VEGFR-2（esVEGFR-2）を発見し，この分子が正常角膜の無リンパ管環境を作るのに重要な役割を演じていることを見出した[1]．なお，esVEGFR-2は膜結合型のVEGFR-2からのsplicing variantで，VEGF-Cの作用を選択的に阻害する[1]．

国立がんセンター・がん対策情報センターによれば（2008年統計）[2]，日本国内で乳癌は癌死亡の第5位で，年齢別にみた女性の乳癌の罹患率は30歳代から増加し，40歳代後半から50歳代前半にピークを迎え，その後は次第に減少傾向を示す．年次推移は罹患率，死亡率ともに増加を示し，出生年代別では最近生まれた人ほど罹患率，死亡率が高い傾向がある．罹患率の国際比較では，東アジアよりも欧米，特にアメリカ白人が高く，アメリカの日本人移民は日本国内在住者より高い傾向

がある．これらの動向には生活様式の欧米化がその一因と考えられており，乳癌発生率の増加は世界的な傾向にある．

乳癌患者の死因の殆どは肺，骨などへの転移によるものであり，癌転移を克服する事こそが延命効果につながると考えられ，癌治療の最大の課題と言える．従って，乳癌の転移抑制に対する低毒性の治療法・化学予防法の開発は急務である．乳癌では，リンパ節転移の有無は重要な予後因子である[3]．転移には，血管を介する血行性転移，リンパ管を介するリンパ行性転移があり，腫瘍内の脈管の発生や新生は癌の増殖や転移に大いに関与していると考えられている[4,5]．これらに関わるシグナル伝達を阻害することが出来れば，転移を抑止することが可能となり，結果として延命効果につながると考えられる．そこで，新規スプライシング・バリアントとして同定されたesVEGFR-2（VEGF-C選択的阻害）[1]を用いて，高転移性マウス乳癌モデルに対して遺伝子治療を施した結果，リンパ節転移を抑制した．本研究成果はBMC Medicine, 8巻, 69, 2010年[6]に掲載され，本稿はそれから抜粋・解説したものである．

材料と方法

1．ベクター

マウス角膜から単離したesVegfr-2遺伝子をpDNA3.1ベクターに組み込み，pesVEGFR-2ベクターを作製した．また，endostatin発現ベクター（pEndo）は陽性対照として用いた[7]．対照群としては，何も遺伝子を挿入していないpDNA3.1ベクターを用いた（pVec）．

2．乳癌細胞株

本実験で用いた乳癌細胞株BJMC3879Luc2は，BALB/c系マウスにMMTVを接種することにより誘発された乳癌より樹立されたBJMC3879細胞株[8]にLuciferase遺伝子を安定的に組み込んだものである[9]．BJMC3879細胞株を同系マウスに移植するとリンパ節や肺に高率に転移を起こす[7,10,11]．

3．In vivo乳癌モデル実験

6週齢の30匹のBALB/c系雌マウス（日本SLC）の鼠径部皮下乳腺部にBJMC3879Luc2細胞を移植し，腫瘍径が0.4～0.5cmになった時点で，pesVEGFR-2，pEndoないしは空ベクター（pVec）を週1回の割合で6週間，腫瘍内に直接，注射し，gene electrotransfer（model CUY21EDIT，ネッパジーン社）を行った．0.6-0.7cmまでの腫瘍に対しては各ベクターのDNA量は最大50 μgまで投与し，それ以上のサイズの腫瘍に対しては75 μgのプラスミドベクターを投与した．electrogene transferの条件は100 Volts，1パルスの長さが20msecで8パルス反復させた．毎週，体重と乳腺腫瘍のサイズを個体別に測定した．乳腺腫瘍はデジタル式キャリパスで短径と長径を計測し，その体積を長径×(短径)^2×0.4の算出式で求めた[12]．実験開始の6週経過後には，全生存動物を屠殺剖検し，乳腺腫瘍を摘出し，10%リン酸緩衝ホルマリン溶液にて固定した．肺およびリンパ節（腋窩部，鼠径大腿部）を採取し，更に肉眼病変部と異常の観察されたリンパ節についても採取し，病理組織学的に詳細に検索した．

4．癌転移の生体イメージング

実験開始の6週時に，マウス1匹当たり3 mgのD-luciferin potassium salts（和光純薬工業）を腹腔内に投与し，イソフルレン吸入麻酔下にて，Photon Imager（Biospace社）[9]を用いて，生体発光イメージングを行い，転移の拡がりを群間で比較した．

5．腫瘍内微小血管およびリンパ管の定量

血管内皮のマーカーであるCD34を抗CD34抗体（Hycult Biothech社）とリンパ管内皮のマーカーであるLyve-1を抗Lyve-1抗体（Acris Antibodies社）を用いて，二重免疫蛍光染色を施した．2つの画像を重ね合わせて，CD34$^+$/Lyve-1$^-$を血管として，CD34$^-$/Lyve-1$^+$をリンパ管として，それぞれの腫瘍内密度を算定した．

6．腫瘍内のリンパ管侵襲の数

Lyve-1の他にリンパ管内皮のマーカーとして，podoplaninを抗podoplanin抗体（AngioBio社）を用いて免疫組織学的染色を施し，癌細胞侵襲を受けた腫瘍内リンパ管の数を算出した．

7．アポトーシスの解析

乳腺腫瘍のパラフィン包埋薄切切片を用いて，3'-OH末端のDNA切断を証明するTUNEL染色（Apoptosis *in situ* Detection Kit，和光純薬工業）を施し，TUNEL陽性細胞数を算定し，腫瘍の単位面積当たりのアポトーシス細胞として算出した．

8．DNA合成の解析

屠殺1時間前に50mg/kgの用量で5-bromo-2'-deoxyuridine（BrdU; Sigma社）を腹腔内に投与した．乳腺腫瘍のパラフィン包埋薄切切片について，抗BrdU抗体（Dako社）を用いて免疫組織染色を施し，BrdUの取り込みの観察されたS期細胞数を算定し，BrdU標識率を腫瘍の単位面積当たりの数として算出した．

9．統計学的解析

対照群と投与群との間の定量的データではStudentの*t*検定を行った．発生頻度の解析にはFisherの正確確